This is a repository copy of *An in vivo platform for identifying inhibitors of protein aggregation*.

Article:

<div align="center">SUPPLEMENTARY INFORMATION</div>

An *in vivo* platform for identifying inhibitors of protein aggregation

Janet C. Saunders[1, 2 †]**, Lydia M. Young**[1, 2 †]**, Rachel A. Mahood**[1, 2]**, Matthew P. Jackson**[1, 2]**, Charlotte H. Revill**[1, 3]**, Richard J. Foster**[1, 3]**, D. Alastair Smith**[4]**, Alison E. Ashcroft**[1, 2]**, David J. Brockwell**[1, 2 *]**, Sheena E. Radford**[1, 2 *]

[†]These authors contributed equally to this work

*Corresponding authors: D.J.Brockwell@leeds.ac.uk and S.E.Radford@leeds.ac.uk

[1]Astbury Centre for Structural Molecular Biology, University of Leeds, Leeds, LS2 9JT, UK. [2]School of Molecular and Cellular Biology, University of Leeds, Leeds, LS2 9JT, UK. [3]School of Chemistry, University of Leeds, LS2 9JT, UK. [4]Avacta Analytical plc, Wetherby, LS23 7FZ, UK

SUPPLEMENTARY TABLES

βla-linker_{SHORT}	DNA	ATGAGTATTC AACATTTCCG TGTCGCCCTT ATTCCCTTTT TTGCGGCATT TTGCCTTCCT GTTTTTGCTC ACCCAGAAAC GCTGGTGAAA GTAAAAGATG CTGAAGATCA GTTGGGTGCA CGAGTGGGTT ACATCGAACT GGATCTCAAC AGCGGTAAGA TCCTTGAGAG TTTTCGCCCC GAAGAACGTT TTCCAATGAT GAGCACTTTT AAAGTTCTGC TATGTGGCGC GGTATTATCC CGTGTTGACG CCGGGCAAGA GCAACTCGGT CGCCGCATAC ACTATTCTCA GAATGACTTG GTTGAGTACT CACCAGTCAC AGAAAAGCAT CTTACGGATG GCATGACAGT AAGAGAATTA TGCAGTGCTG CCATAACCAT GAGTGATAAC ACTGCGGCCA ACTTACTTCT GACAACGATC GGAGGACCGA AGGAGCTAAC CGCTTTTTTG CACAACATGG GGGATCATGT AACTCGCCTT GATCGTTGGG AACCGGAGCT GAATGAAGCC ATACCAAACG ACGAGCGTGA CACCACGATG CCTGCAGCAA TGGCAACAAC GTTGCGCAAA CTATTAACTG GCGAACTA**GG TGGTGGTGGT TCTGGTGGTG GTGG**CTCGAG CTCA**GGATCC GGGAGCGGTT** **CCGGAAGCGG AGGAGGTGGT TCAGGCGGAG GTGGAAGC**TT GACTCTAGCT AGCCGGCAGC AGCTCATAGA CTGGATGGAG GCGGATAAAG TTGCAGGACC ACTTCTGCGC TCGGCCCTTC CGGCTGCTG GTTATTGCT GATAAATCTG GAGCCGGTGA GCGTGGGTCT CGCGGTATCA TTGCAGCACT GGGGGCCAGAT GGTAAGCCCT CCCGTATCGT AGTTATCTAC ACGACGGGGA GTCAGGCAAC TATGGATGAA CGAAATAGAC AGATCGCTGA GATAGGTGCC TCACTGATTA AGCATTGG<u>TA</u> <u>A</u>
	Amino acid	MSIQHFRVAL IPFFAAFCLP VFAHPETLVK VKDAEDQLGA RVGYIELDLN SGKILESFRP EERFPMMSTF KVLLCGAVLS RVDAGQEQLG RRIHYSQNDL VEYSPVTEKH LTDGMTVREL CSAAITMSDN TAANLLLTTI GGPKELTAFL HNMGDHVTRL DRWEPELNEA IPNDERDTTM PAAMATTLRK LLTGEL**GGGG SGGGGSSSGS GSGSGSGGGG SGGGGS**LTLA SRQQLIDWME ADKVAGPLLR SALPAGWFIA DKSGAGERGS RGIIAALGPD GKPSRIVVIY TTGSQATMDE RNRQIAEIGA SLIKHW
βla-linker_{LONG}	DNA	ATGAGTATTC AACATTTCCG TGTCGCCCTT ATTCCCTTTT TTGCGGCATT TTGCCTTCCT GTTTTTGCTC ACCCAGAAAC GCTGGTGAAA GTAAAAGATG CTGAAGATCA GTTGGGTGCA CGAGTGGGTT ACATCGAACT GGATCTCAAC AGCGGTAAGA TCCTTGAGAG TTTTCGCCCC GAAGAACGTT TTCCAATGAT GAGCACTTTT AAAGTTCTGC TATGTGGCGC GGTATTATCC CGTGTTGACG CCGGGCAAGA GCAACTCGGT CGCCGCATAC ACTATTCTCA GAATGACTTG GTTGAGTACT CACCAGTCAC AGAAAAGCAT CTTACGGATG GCATGACAGT AAGAGAATTA TGCAGTGCTG CCATAACCAT GAGTGATAAC ACTGCGGCCA ACTTACTTCT GACAACGATC GGAGGACCGA AGGAGCTAAC CGCTTTTTTG CACAACATGG GGGATCATGT AACTCGCCTT GATCGTTGGG AACCGGAGCT GAATGAAGCC ATACCAAACG ACGAGCGTGA CACCACGATG CCTGCAGCAA TGGCAACAAC GTTGCGCAAA CTATTAACTG GCGAACTA**GG TGGTGGTGGT TCTGGTGGTG GTGGTTCTTC CTCAGGTTCA GGTGGCGGGG** **GATCTGGTGG TGGTGGCTCA** GGATCCGGTG G**CTCGAG**TTC CGGGAGCGGG AGCTCTTCTG GTTCCGGAGG CGGTGGAGGA **TCAGGCGGTG GCGGATCAGG AAGTGGGAGC GGAGGCGGCG GATCAGGCGG AGGTGGAAGC**TTGACTCTAG CTAGCCGGCA GCAGCTCATA GACTGGATGG AGGCGGATAA AGTTGCAGGA CCACTTCTGC GCTCGGCCCT TCCGGCTGGC TGGTTTATTG CTGATAAATC TGGAGCCGGT GAGCGTGGGT CTCGCGGTAT CATTGCAGCA CTGGGGCCAG ATGGTAAGCC CTCCCGTATC GTAGTTATCT ACACGACGGG GAGTCAGGCA ACTATGGATG AACGAAATAG ACAGATCGCT GAGATAGGTG CCTCACTGAT TAAGCATTGG <u>TAA</u>
	Amino acid	MSIQHFRVAL IPFFAAFCLP VFAHPETLVK VKDAEDQLGA RVGYIELDLN SGKILESFRP EERFPMMSTF KVLLCGAVLS RVDAGQEQLG RRIHYSQNDL VEYSPVTEKH LTDGMTVREL CSAAITMSDN TAANLLLTTI GGPKELTAFL HNMGDHVTRL DRWEPELNEA IPNDERDTTM PAAMATTLRK LLTGEL**GGGG SGGGGSSSGS GGGGSGGGGS GSGGSSSGSG SSSGSGGGGG** **SGGGGSGSGS GGGGSGGGGS** LTLASRQQLI DWMEADKVAG PLLRSALPAG WFIADKSGAG ERGSRGIIAA LGPDGKPSRI VVIYTTGSQA TMDERNRQIA EIGASLIKHW

Supplementary Table 1. DNA and amino acid sequences of β-lactamase constructs. The periplasmic signal sequence is in purple. The 28-residue (βla-linker_{SHORT}) and 64-residue (βla-linker_{LONG}) G/S-rich linker is shown in bold. The restriction sites XhoI and BamHI are shown in blue and green, respectively. The start and stop codons are underlined.

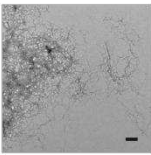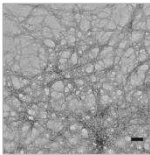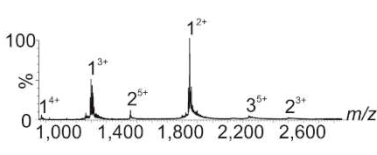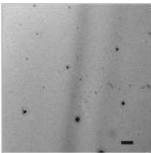| Primer	Sequence	Purpose
IAPP-Forward	CGCATTACTTGTCTCGAGCAAATGCAACACCGCGACC	Addition of XhoI restriction site 5' of hIAPP or rIAPP gene to clone it into β-lactamase linker
IAPP-Reverse	CGCATTACTGTAGGATCCATAGGTGTTGCTGCCCAC	Addition of BamHI restriction site 3' of hIAPP or rIAPP gene to clone it into βla-linker$_{SHORT}$
Aβ42-Forward	CGCATTACTTGTCTCGAGCGATGCGGAGTTCCGTCATG	Addition of XhoI restriction site 5' of Aβ42 gene to clone it into βla-linker$_{SHORT}$
Aβ42-Reverse	CGCATTTCTGTAGGATCCCGCTATGACAACACCACC	Addition of BamHI restriction site 3' of Aβ42 gene to clone it into βla-linker$_{SHORT}$
HEL4/Dp47d-Forward	CGCATTACTTGTCTCGAGCGAAGTGCAGCTGCTGGAAAGC	Addition of XhoI restriction site 5' of HEL4 or Dp47d gene to clone it into β-lactamase linker
HEL4/Dp47d-Reverse	CGCATTAATATAGGATCCGCTGCTCACGGTCACCAG	Addition of BamHI restriction site 3' of HEL4 or Dp47d gene to clone it into βla-linker$_{SHORT}$
β$_2$m-Forward	CGCACTTGCCTCGAGCATGATTCAAAG	Addition of XhoI restriction site 5' of human β$_2$m gene to clone it into β-lactamase linker
β$_2$m-Reverse	CATTACTAGAGGATCCGTCTCGATCCCA	Addition of BamHI restriction site 3' of human β$_2$m gene to clone it into βla-linker$_{SHORT}$
β$_2$m D76N-Forward	CACTGAAAAAAATGAGTATGCC	Convert human β$_2$m to human β$_2$m D76N
β$_2$m D76N-Reverse	GGGGTGAATTCAGTGTAG	
Aβ40- Forward	GGATCCGGGAGCGGTTCC	Convert βla-Aβ42 to βla-Aβ40
Aβ40- Reverse	GACAACACCACCCACCATG	
βLA linker Forward	CGGAGCTGAATGAAGCCATACC	Sequence the G/S linker of βla-linker$_{SHORT}$ to ensure correct insertion of guest protein
βLA linker Reverse	TCACCGGCTCCAGATTTATCAGC	

Supplementary Table 2. Oligonucleotide primers. The restriction enzyme recognition sites are highlighted in blue (XhoI) and green (BamHI).

SUPPLEMENTARY RESULTS

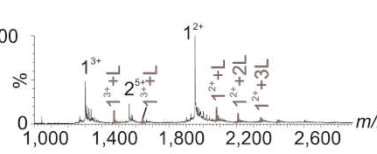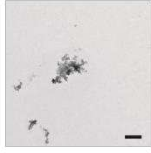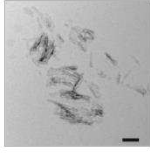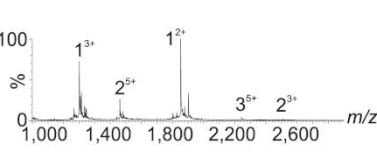| Molecule	Mode of Inhibition
Curcumin (1)	Significantly reduces hIAPP aggregation *in vitro* and alleviates some toxicity of pancreatic β-cells *in vivo*[1].
Acid fuchsin (2)	Inhibits all amyloid formation at 10:1 molar ratio of acid fuchsin: hIAPP[2]. Arrests amyloid formation by trapping intermediate species[3].
EGCG (3)	Potent inhibitor of hIAPP aggregation[4-8]; can disaggregate amyloid fibrils[9].
Fast green FCF (4)	10:1 molar ratio of Fast green FCF: hIAPP inhibits all aggregation[2, 8].
Caffeic acid (6)	5:1 molar ratio of caffeic acid: hIAPP inhibits all aggregation[10].
Silibinin (16)	Results in amorphous aggregates/fibrillar material at 5:1 molar ratio of silibinin: hIAPP[11], and complete inhibition of amyloid formation at 10:1 molar ratio[4].
Acridine orange (5)	20-fold molar excess used for inhibition, however only ThT fluorescence data shown (no TEM)[12].
Myricetin (7)	Low ThT fluorescence observed in presence of myricetin, but no analyses of aggregates performed[13]. Aggregate inhibition occurred for 45 min at a 10:1 molar ratio of myricetin: hIAPP by AFM[14], however no effect found in another study[15].
Phenol Red (8)	10:1 molar ratio of phenol red: hIAPP leads to small reduction in fibril formation[16], potentially binds and improves solubility of early protofibrils[17].
Morin hydrate (17)	10:1 molar ratio of morin hydrate: hIAPP leads to formation of short fibrils and amorphous aggregates[15].
Hemin (9)	No effect: fibrils formed at 10:1 molar ratio of hemin: hIAPP[8].
Resveratrol (10)	Slows, but does not prevent, hIAPP amyloid formation at high concentrations (20:1 molar ratio)[18].
1*H*-B-SA (11)	No effect: fibrils formed at 10:1 molar ratio of 1*H*-B-SA: hIAPP[8].
Benzimidazole (13)	No effect: fibrils formed at 10:1 molar ratio of benzimidazole: hIAPP[8].
Tramiprosate (15)	No effect[3]; fibrils formed at 10:1 molar ratio of tramiprosate: hIAPP[3, 8].
Aspirin (18)	No effect: fibrils formed at 10:1 molar ration of hemin: hIAPP[8].
Congo red (20)	Colloidal inhibition of fibril formation at 10:1 molar ratio of Congo red: hIAPP[8, 19, 20].
Azure A (12)	No effect: fibrils formed at 10:1 molar ratio of Azure A: hIAPP (unpublished data).
Thiabendazole (14)	No effect: fibrils formed at 10:1 molar ratio of thiabendazole: hIAPP (unpublished data).
Orange G (19)	Colloidal inhibition of fibril formation at 10:1 molar ratio of Orange G: hIAPP (unpublished data).

Supplementary Table 3. Mode of hIAPP aggregation inhibition by small molecules. Well-characterized inhibitors are highlighted in green, small molecules known not to prevent hIAPP aggregation are highlighted in red. The four molecules with inconclusive published data are highlighted in blue. Compound number is given in brackets.

Small molecule (N°)	*In vivo* classification	TEM		ThT fluorescence	Mass spectrum	Binding mode and max oligomers observed by ESI-IMS-MS	
		500 nm	100 nm				
-	-			Yes		-	6
Curcumin (1)	Hit			No		Positive	3
Acid fuchsin (2)	Hit			No		Positive	1
EGCG (3)	Hit			No		Positive	1
Fast Green FCF (4)	Hit			No		Positive	1
Acridine Orange (5)	Hit			No		Positive	3
Caffeic acid (6)	Hit			No		Negative	5
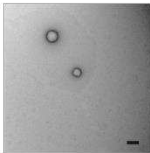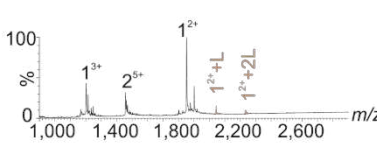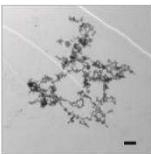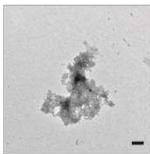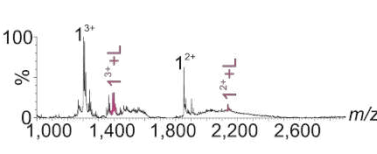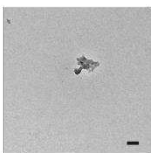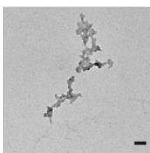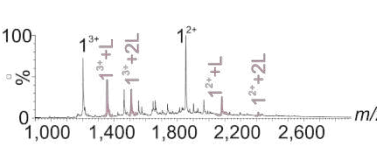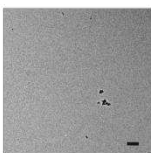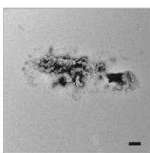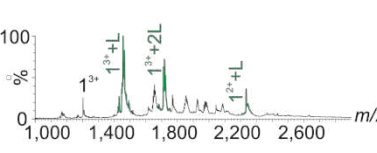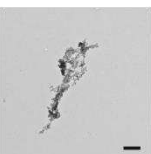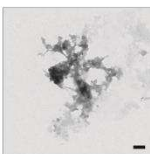
Supplementary Table 4. *In vitro* analysis of hIAPP aggregation in presence or absence of small molecules. Negative stain TEM was performed after five days incubation (25 °C, quiescent) of a 10:1 molar ratio of small molecule: protein (320:32 μM). Scale bars = 500 and 100 nm. ThT fluorescence data (25 h measurement; enhancement in fluorescence = yes, no effect = no) are included to highlight issues with using this technique for small molecule screening[21]. Positive ion ESI mass spectra. Labels X^{y+} denote the oligomer order (X) and charge state of the species (y+). $X^{y+} + nL$ denotes the number (n) of ligands (L) bound to the particular X^{y+} charge state. Binding mode as determined from the mass spectra is denoted as positive, negative, non-specific or colloidal[8]. Maximum number of oligomers observed using ESI-IMS-MS is indicated.

Small molecule (N°)	In vivo classification	TEM 500 nm	TEM 100 nm	ThT fluorescence	Mass spectrum	Binding mode and max oligomers observed by ESI-IMS-MS	
Myricetin (7)	Inconclusive			No (false-positive)		Non-specific/ colloidal	3
Phenol red (8)	Inconclusive			No (false positive)		Non-specific	2
Hemin (9)	Negative			Yes		Negative	6
Resveratrol (10)	Negative			No (false-positive)		Negative	3
1H-B-SA (11)	Negative			No (false positive)		Non-specific	1
Azure A (12)	Negative			No (false positive)		Negative	5
Benimidazole (13)	Negative			No (false positive)		Negative	6
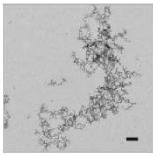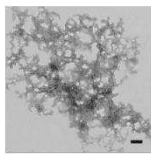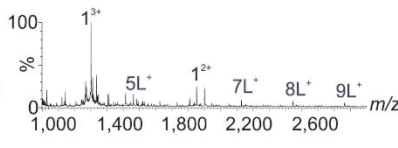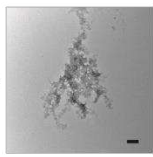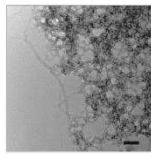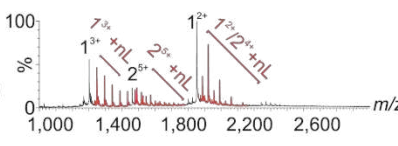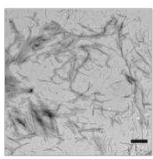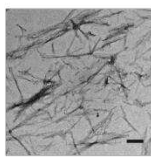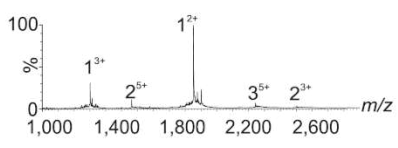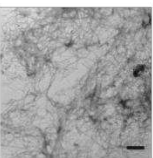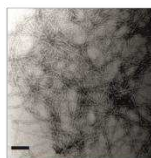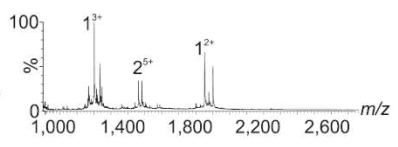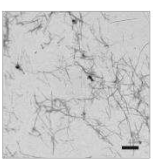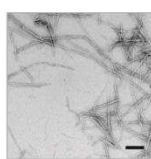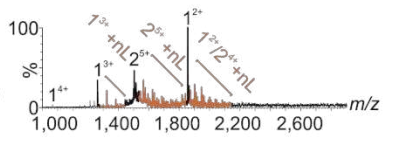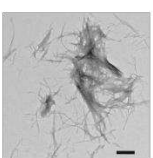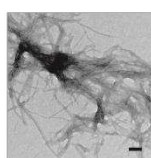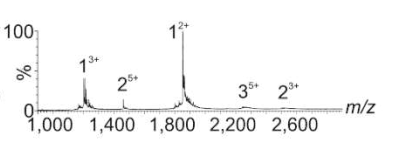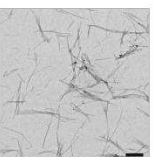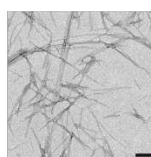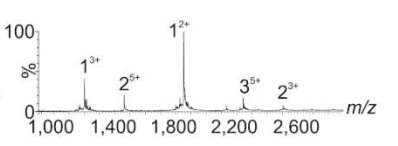
Supplementary Table 4. *In vitro* analysis of hIAPP aggregation in presence or absence of small molecules. Negative stain TEM was performed after five days incubation (25 °C, quiescent) of a 10:1 molar ratio of small molecule: protein (320:32 μM). Scale bars = 500 and 100 nm. ThT fluorescence data (25 h measurement; enhancement in fluorescence = yes, no effect = no) are included to highlight issues with using technique for small molecule screening[21]. Positive ion ESI mass spectra. Labels X^{y+} denote the oligomer order (X) and charge state of the species (y+). X^{y+} + nL denotes the number (n) of ligands (L) bound to the particular X^{y+} charge state. Binding mode as determined from the mass spectra is denoted as positive, negative, non-specific or colloidal. Maximum number of oligomers observed using ESI-IMS-MS is indicated.

6

Small molecule (N°)	In vivo classification	TEM		ThT fluorescence	Mass spectrum	Binding mode and max oligomers observed by ESI-IMS-MS	
		500 nm	100 nm				
Thiabendazole (14)	Negative			No (false positive)		Negative	4
Tramiprosate (15)	Negative			No (false positive)		Non-specific	1
Silibinin (16)	Negative			No		Positive	1
Morin hydrate (17)	Negative			No (false positive)		Negative	4
Aspirin (18)	Negative			Yes		Negative	6
Orange G (19)	Negative			No (false positive)		Colloidal	1
Congo red (20)	Colloidal			No (false positive)		Colloidal	1
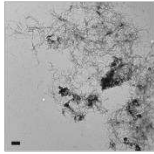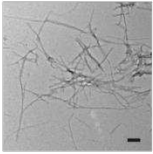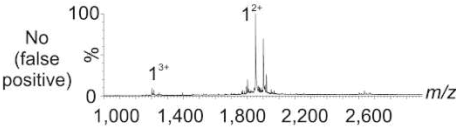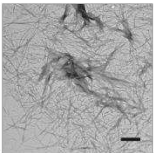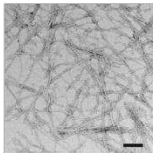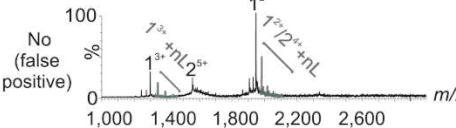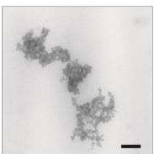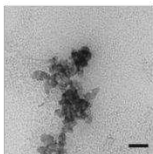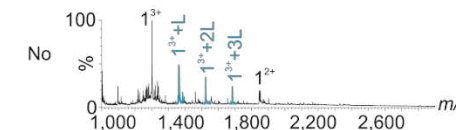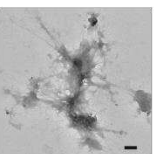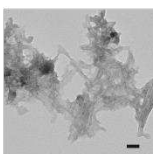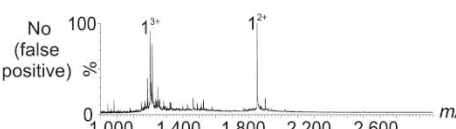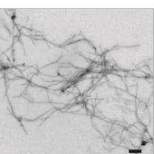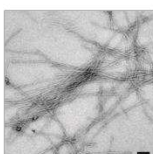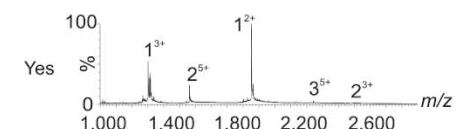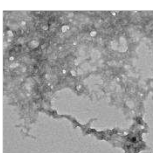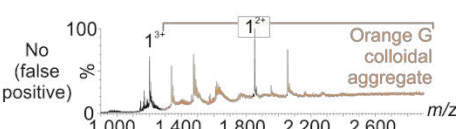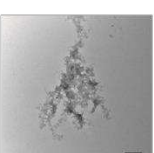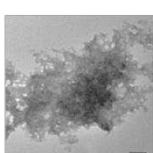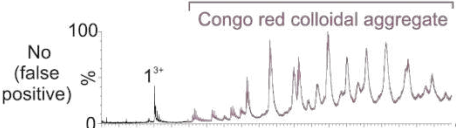
Supplementary Table 4. *In vitro* analysis of hIAPP aggregation in presence or absence of small molecules. Negative stain TEM was performed after five days incubation (25 °C, quiescent) of a 10:1 molar ratio of small molecule: protein (320:32 μM). Scale bars = 500 and 100 nm. ThT fluorescence data (25 h measurement; enhancement in fluorescence = yes, no effect = no) are included to highlight issues with using technique for small molecule screening[21]. Positive ion ESI mass spectra. Labels X^{y+} denote the oligomer order (X) and charge state of the species (y+). $X^{y+} + nL$ denotes the number (n) of ligands (L) bound to the particular X^{y+} charge state. Binding mode as determined from the mass spectra is denoted as positive, negative, non-specific or colloidal. Maximum number of oligomers observed using ESI-IMS-MS is indicated.

Supplementary Figures

a

```
             1        10        20        30        40
Aβ1-42  (M)DAEFRHDSGYEVHHQKLVFFAEDVGSNKGAIIGLMVGGVVIA
```

```
             1        10        20        30
hIAPP      KCNTATCATQRLANFLVHSSNNFGAILSSTNVGSNTY-NH2
             *     *
```

```
             1        10        20        30
rIAPP      KCNTATCATQRLANFLVRSSNNLGPVLPPTNVGSNTY-NH2
             *     *
```

b

```
             1        10        20        30        40
Aβ1-42  (M)DAEFRHDSGYEVHHQKLVFFAEDVGSNKGAIIG-LMVGGVVIA
                        ::  ::  |  ||  ::::  :  |||  :  ||
hIAPP      -----KCNTATCATQRLANFLVHSSNNFGAILSSTNVGSNTY-NH2
                1*       *  10        20        30
```

Supplementary Figure 1. Protein sequences of Aβ40/42, hIAPP and rIAPP. (**a**) Amino acid sequences of Aβ40/42, hIAPP and rIAPP. The additional two C-terminal residues in Aβ42 are highlighted in green. Recombinant expression of the peptide Aβ40 results in an additional N-terminal methionine[22] (synthetic Aβ42 used herein lacks this additional residue). The residues in rIAPP that differ in hIAPP are highlighted in blue and the amidated C-terminus is shown. (**b**) Sequence alignment of a 37-residue overlap of hIAPP and Aβ42. Lines indicate exact amino acid matches, dashes indicate chemical similarity. All cysteine residues that form intramolecular disulfide bonds are indicated by asterisks.
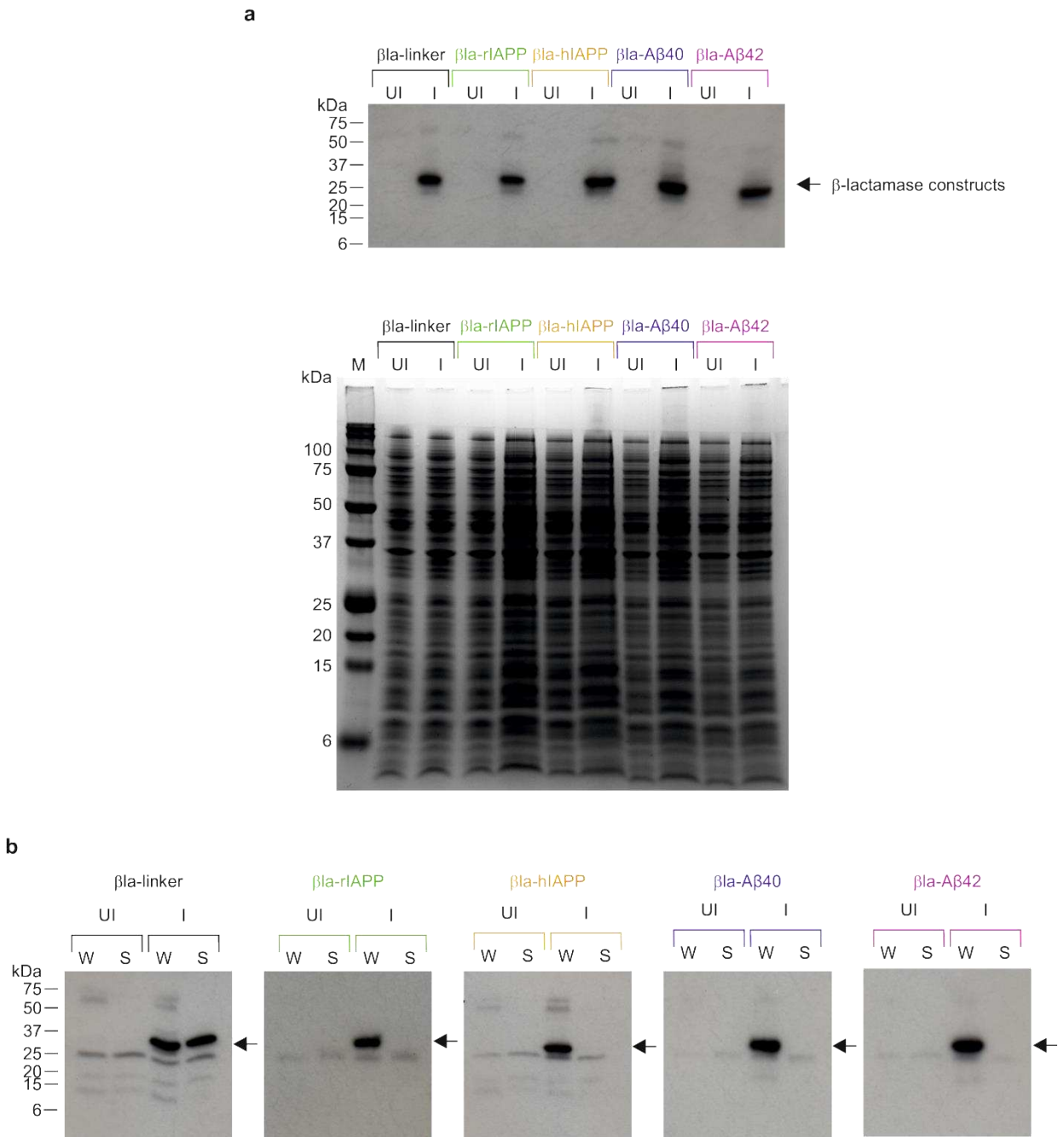
Supplementary Figure 2. Expression level and solubility of β-lactamase constructs *in vivo*. (**a**, top) Western blot analysis of βla-linker (black), βla-rIAPP (green), βla-hIAPP (orange), βla-Aβ40 (purple) or βla-Aβ42 (pink) expression levels. Black arrow indicates β-lactamase constructs. UI = uninduced sample, I = samples after 1 h induction of protein expression. (**a**, bottom) SDS-PAGE loading control. (**b**) Comparison of the amount of β-lactamase construct in the whole (W) versus the soluble (S) fraction, before (UI) and after (I) 1 h induction of protein expression. Soluble samples were obtained by lysis of the cells using bacterial protein extraction reagent[TM], followed by centrifugation of the samples to remove the insoluble fraction (16,000 *g*, 30 min, 4 °C).

a

b

c

d
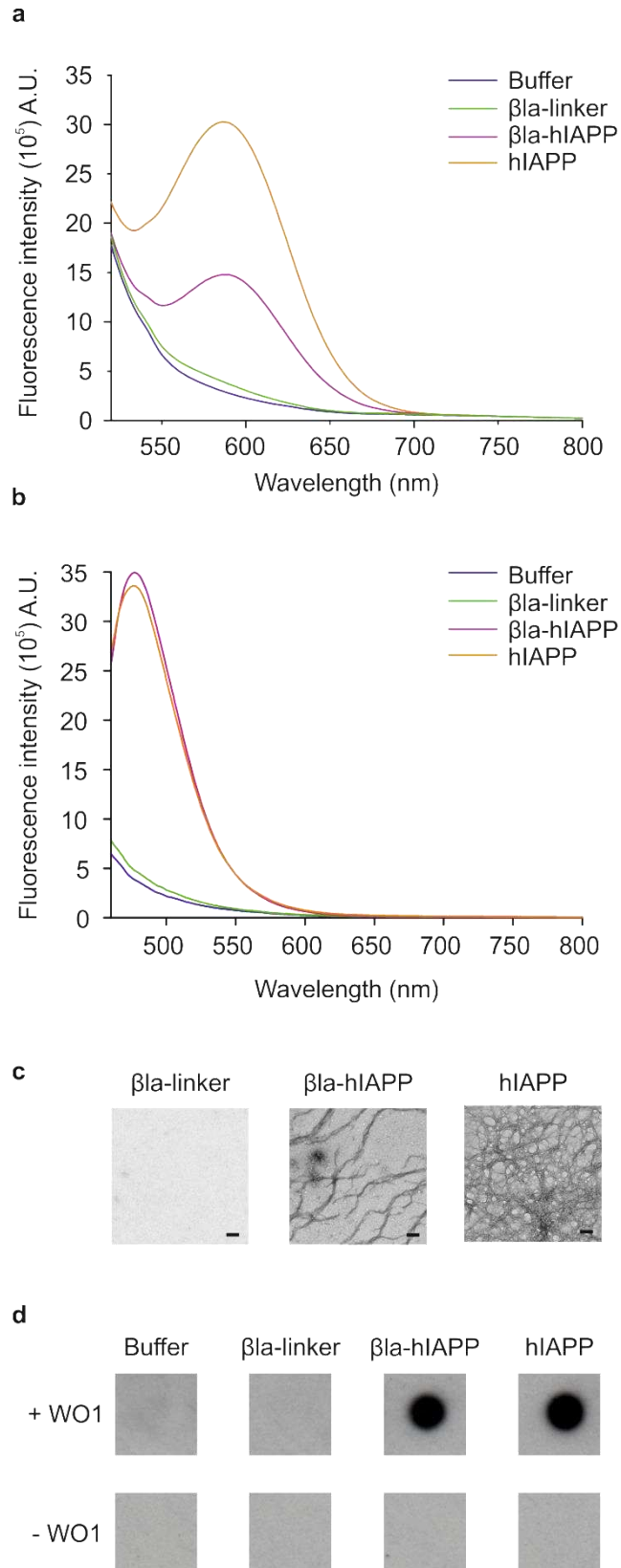
Supplementary Figure 3. βla-hIAPP aggregates into amyloid-like fibrils. Fluorescent emission spectra of 50 μM βla-linker, βla-hIAPP or hIAPP in the presence of 10 μM (**a**) NIAD-4 or (**b**) ThT after 5 days incubation (pH 6.8, quiescent, 25 °C). (**c**) Negative stain TEM images of βla-linker, βla-hIAPP and hIAPP peptide (scale bar = 100 nm). (**d**) WO1 dot-blot of 10 μL of 50 μM βla-linker, βla-hIAPP or hIAPP after 5 days incubation (pH 6.8, quiescent, 25 °C).

a

Human
β₂m

```
          1        10        20        30        40        50        60
          IQRTPKIQVYSRHPAENGKSNFLNCYVSGFHPSDIEVDLLKNGERIEKVEHSDLSFSKDW
                                 *
                   70        80        90
          SFYLLYYTEFTPTEKDEYACRVNHVTLSQPKIVKWDRDM
                            *
```

D76N
β₂m

```
          1        10        20        30        40        50        60
          IQRTPKIQVYSRHPAENGKSNFLNCYVSGFHPSDIEVDLLKNGERIEKVEHSDLSFSKDW
                                 *
                   70        80        90
          SFYLLYYTEFTPTEKNEYACRVNHVTLSQPKIVKWDRDM
                            *
```

b

HEL4

```
          1        10        20        30        40        50  a    60
          EVQLLESGGGLVQPGGSLRLSCAASGFRISDEDMGWVRQAPGKGLEWVSSIYGPSGSTYYA
                              *
                   70        80  abc       90  100abc        110
          DSVKGRFTISRDNSKNTLYLQMNSLRAEDTAVYYCASALEPLSEPLGFWGQGTLVTVSS
                                                *
```

Dp47d

```
          1        10        20        30        40        50  a    60
          EVQLLESGGGLVQPGGSLRLSCAASGFTFSSYAMSWVRQAPGKGLEWVSAISGSGGSTYYA
                              *
                   70        80  abc       90  100abc        110
          DSVKGRFTISRDNSKNTLYLQMNSLRAEDTAVYYCAKSYGA----FDYWGQGTLVTVSS
                                                *
```

c

d

Supplementary Figure 4. Antibiotic resistance phenotype conferred to *E. coli* by the globular proteins WT β₂m, β₂m D76N, HEL4 and Dp47d. (**a**) Amino acid sequences of human β₂m and the variant D76N. The single residue difference is highlighted in purple. (**b**) Amino acid sequences of HEL4 and Dp47d. Residues numbered according to Kabat *et al.*[23] (standardized numbering of residues in an antibody). Residues that differ in Dp47d are highlighted in orange. All cysteine residues that form intramolecular disulfide bonds are indicated by asterisks. (**c–d**) Antibiotic survival curves of the maximal cell dilution allowing growth (MCD$_{GROWTH}$) after 18 h over a range of ampicillin concentrations for the larger tripartite fusion constructs. (**c**) MCD$_{GROWTH}$ of bacteria expressing βla-β₂m-WT (purple) or βla-β₂m-D76N (pink) from 0 – 280 µg/mL ampicillin. (**d**) MCD$_{GROWTH}$ of bacteria expressing βla-HEL4 (orange) or βla-Dp47d (teal) from 0 – 140 µg/mL ampicillin. Data represent mean values ± s.e.m (n = 4 replicate experiments).
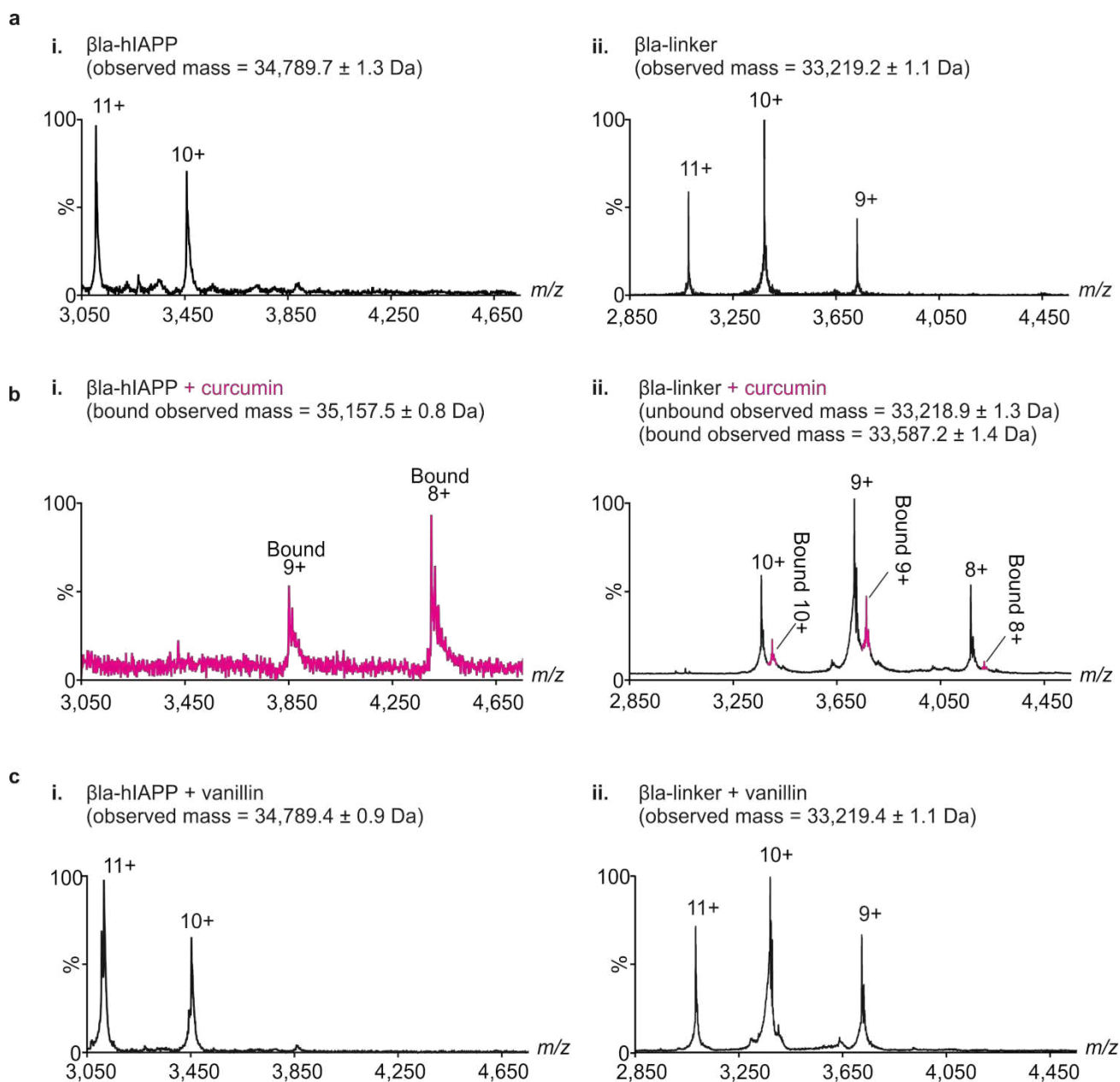
Supplementary Figure 5. Binding of small molecules to βla-hIAPP. (**a**) ESI mass spectrum of βla-hIAPP (**i**) and βla-linker (**ii**) (50 μM protein, 200 mM ammonium acetate, pH 6.8). The numbers above the peaks denote the charge state of each ion. (**b**) ESI mass spectrum of a 10:1 molar ratio (500:50 μM) of curcumin: βla-hIAPP (**i**) or βla-linker (**ii**). The expected mass of βla-hIAPP and βla-linker are 34789.1 Da and 33218.9 Da, respectively. The mass of curcumin is 368 Da. Note: βla-hIAPP is 100 % bound by curcumin and the masses observed correspond to a 1:1 βla-hIAPP: curcumin complex. The charge state distribution of βla-hIAPP shifts to a higher *m/z* when bound to curcumin, suggestive of either a structural compaction, or masking of protonation sites on βla-hIAPP by binding of curcumin. Some binding to βla-linker is also observed (**ii**). (**c**) ESI mass spectrum of a 10:1 molar ratio of vanillin (152 Da), a compound that does not interact with hIAPP. No binding to βla-hIAPP (**i**) or βla-linker (**ii**) is observed.

a

	Non-toxic positive: Acid fuchsin	Toxic positive: Curcumin	Non-toxic negative: Hemin	Toxic negative: Orange G
i. SM effect on bacterial growth ● βla-linker ● βla-linker + SM				
ii. SM effect on protein aggregation ● βla-hIAPP ● βla-hIAPP + SM				
iii. Corrected SM effect on protein aggregation ● βla-hIAPP ● βla-hIAPP + SM corrected				
iv. Growth rescue (% of βla-linker)	22.8 %	28.6 %	-5.7 %	-22.9 %
v. $Log_2 \left(\dfrac{Treated}{Untreated} \right)$	0.37	0.45	-0.11	-0.51
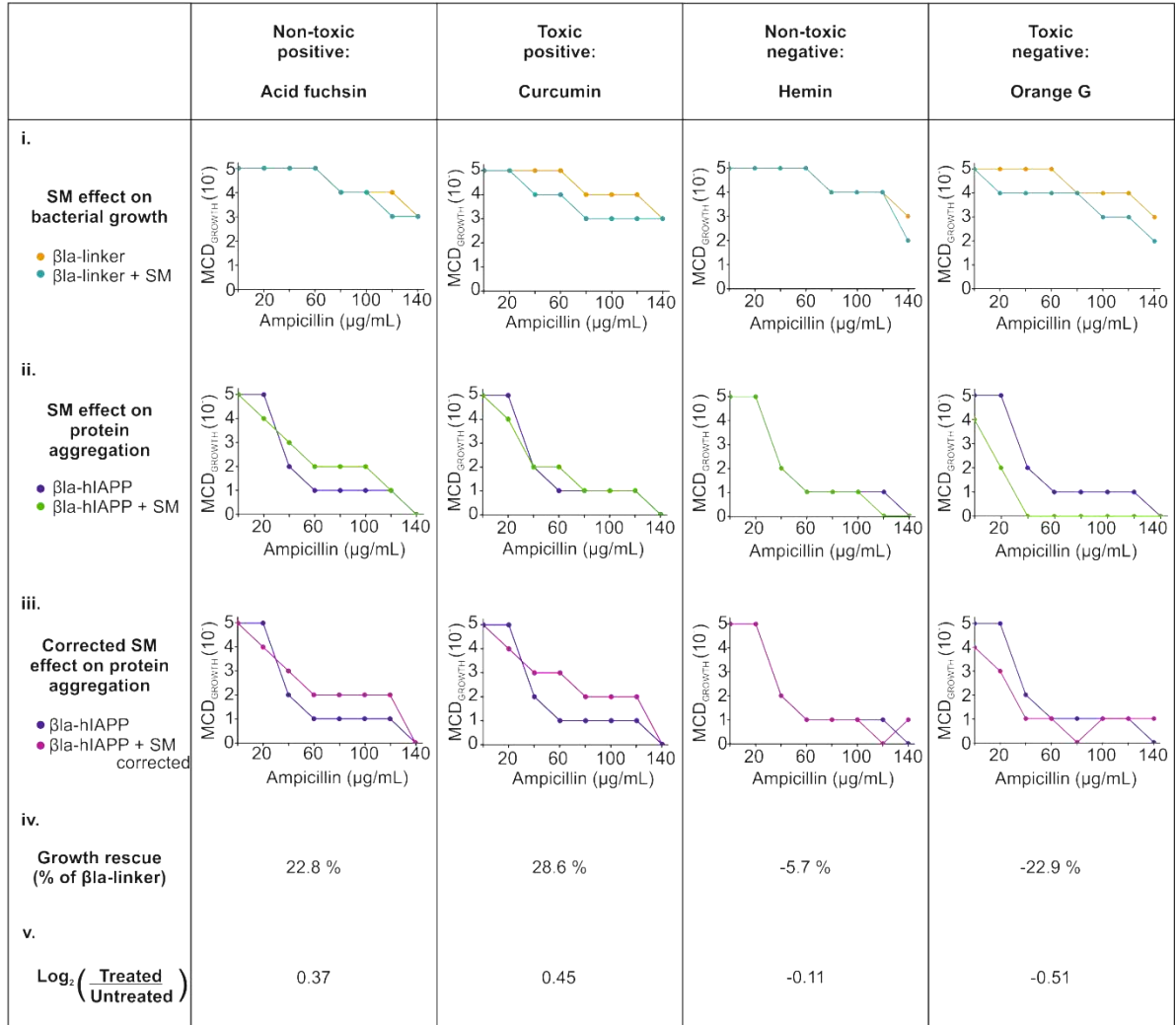
b

Example toxicity calculations for curcumin

	Ampicillin (μg/mL)	
	0	20	40	60	80	100	120	140	
(βla-linker + SM) - (βla-linker)	0	0	-1	-1	-1	-1	-1	0	Δ MCD$_{GROWTH}$ (10^7)
βla-hIAPP + SM	5	4	2	2	1	1	1	0	
βla-hIAPP + SM corrected	5	4	3	3	2	2	2	0	

Supplementary Figure 6. Correcting for intrinsic effects of small molecules (SM) on bacterial growth. (**a**) Data for a non-toxic positive (acid fuchsin), a toxic positive (curcumin), a non-toxic negative (hemin) and a toxic negative (Orange G). (**i**) Intrinsic effect of SM alone on bacterial growth. Maximal cell dilution allowing growth (MCD$_{GROWTH}$) of bacteria expressing βla-linker was assessed at each ampicillin concentration in the absence (●) or presence (●) of 100 μM SM. (**ii**) MCD$_{GROWTH}$ of bacteria expressing βla-hIAPP in the absence (●) or presence (●) of 100 μM SM. (**iii**) The effect of the SM on bacterial growth is corrected at each ampicillin concentration (SM corrected) as the difference between growth in the presence and absence of the SM (●). (**iv**) Bacterial growth rescue as a percentage of βla-linker (area under the curve of βla-hIAPP in the absence of SM = 0 %, area under the curve of βla-linker in the absence of SM = 100 %). (**v**) βla-hIAPP data quantified by log$_2$ (treated MCD$_{GROWTH}$ /untreated MCD$_{GROWTH}$). (**b**) Example data for curcumin (Δ MCD$_{GROWTH}$).
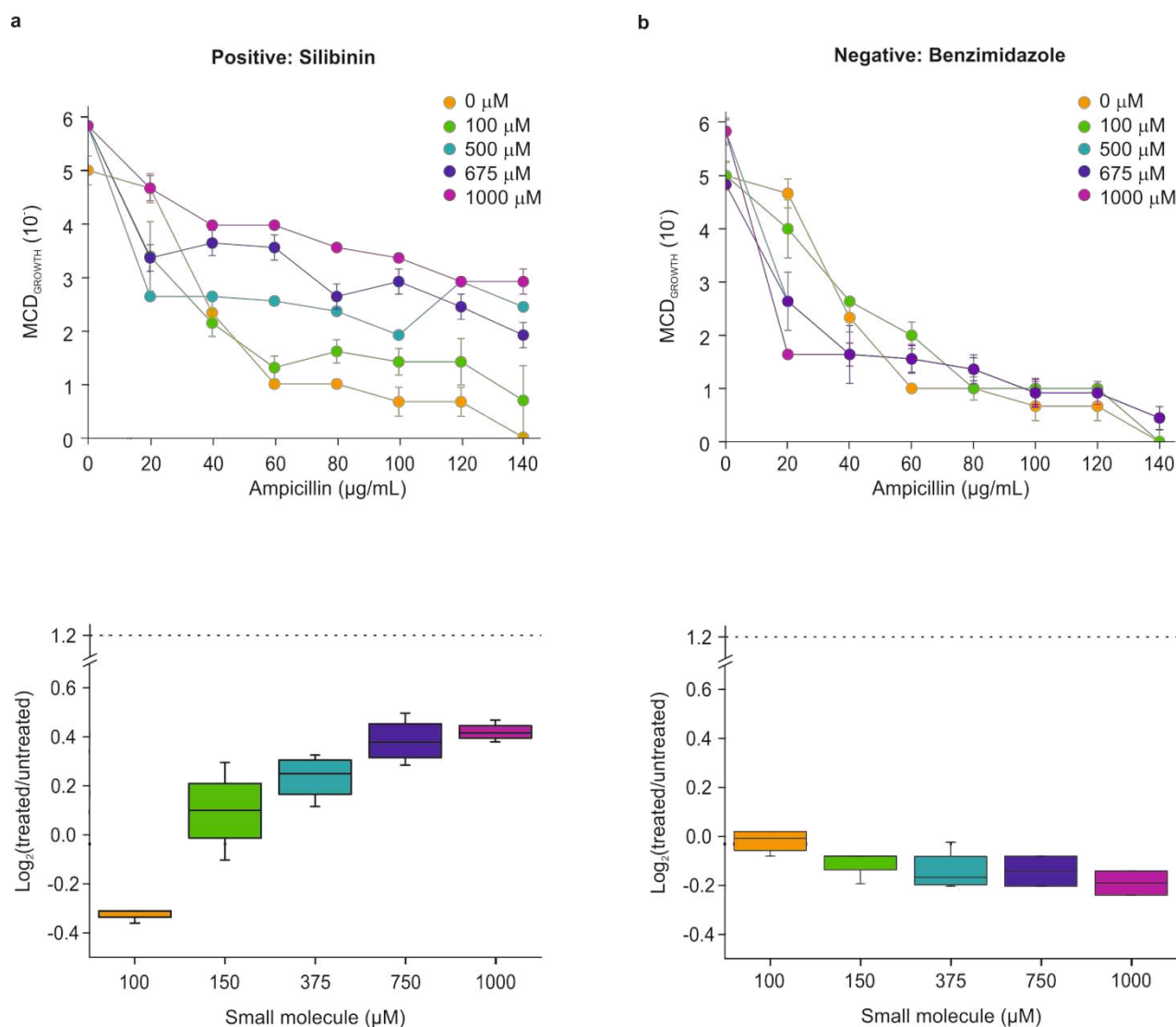
Supplementary Figure 7. Effect of increasing concentrations of silibinin and benzimidazole on bacterial growth. (top) Antibiotic survival curve showing the effect of (**a**) silibinin or (**b**) benzimidazole on growth of bacteria expressing the βla-hIAPP construct. Maximal cell dilution allowing growth (MCD_{GROWTH}) was scored over a range of ampicillin concentrations in the presence of increasing concentrations of small molecule (0-1,000 μM), n = 4 replicate experiments. Data were plotted after the toxicity of the small molecule was accounted for by analysis of the effect of each concentration of small molecule on the growth of cells expressing βla-linker (see online Methods and **Supplementary Fig. 6**). (bottom) (**a**) Silibinin and (**b**) benzimidazole data plotted as $\log_2$ (treated MCD_{GROWTH} /untreated MCD_{GROWTH}) (n = 4 replicates). Data were calculated from the areas under the antibiotic survival curves, after toxicity of small molecule on bacterial growth was accounted for by analysis of the effect of each small molecule on the growth of cells expressing βla-linker. Center line = median; box limits = 25th and 75th percentiles (whiskers extending to ± 1.5 x IQR). Note that in this format (full ampicillin concentration range), 100 % rescue of bacterial growth is equivalent to $\log_2$(treated/untreated) = 1.2 (indicated by dotted line).
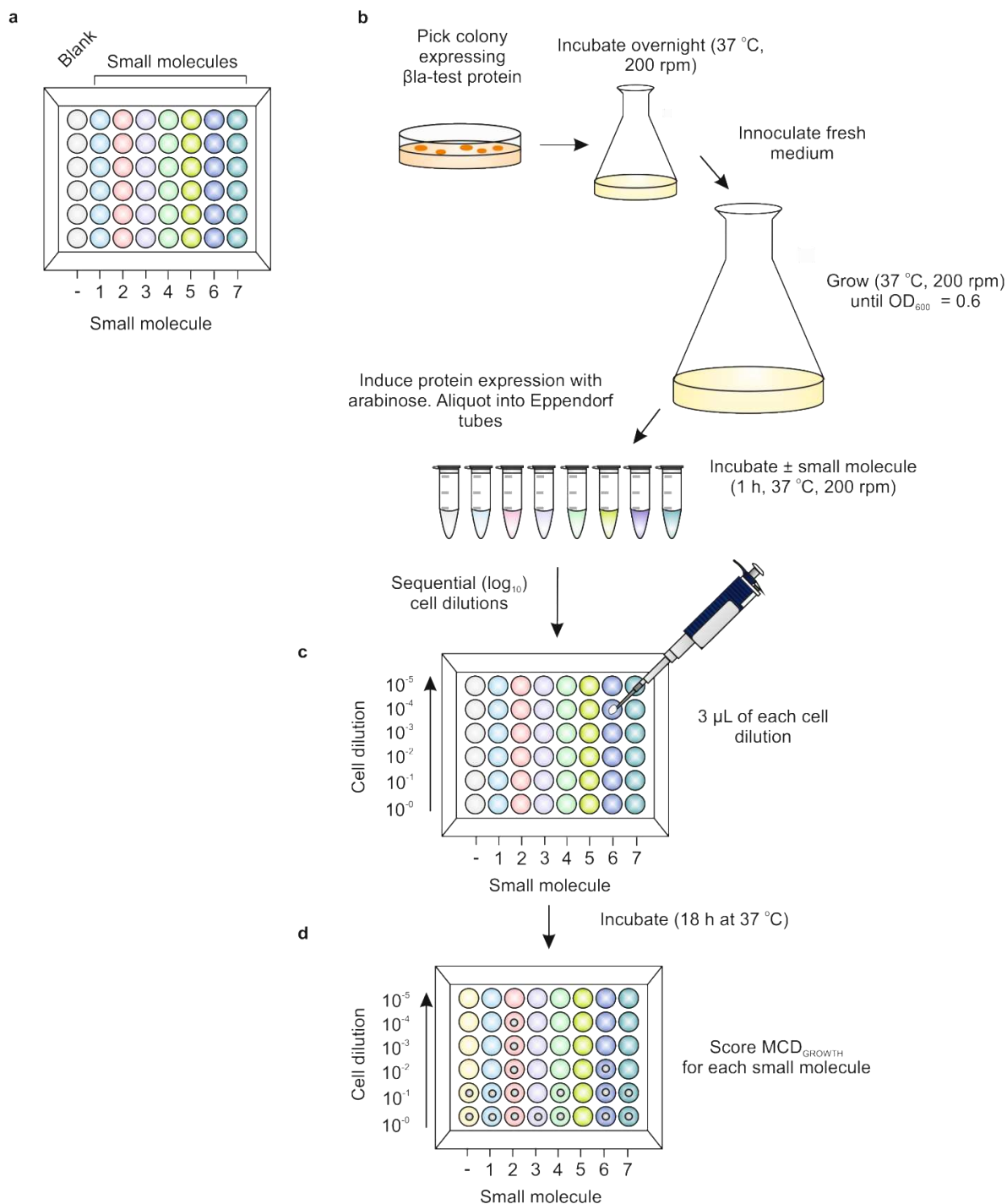
Supplementary Figure 8. Schematic for the miniaturized *in vivo* assay. (**a**) 48-well agar plates, containing a selection of small molecules (1-7) (or blank; -) are prepared prior to performing the assay. (**b**) Colonies transformed with the required plasmid are selected and grown until an OD_{600} of 0.6 is reached. βla-test protein expression is induced with 0.02 % (*w/v*) arabinose and cultures are pre-incubated in the presence or absence of small molecule for 1 h. (**c**) Cultures are serially diluted and 3 μL pipetted onto each well of the prepared agar plates. Plates are incubated for 18 h at 37 °C. (**d**) The maximal cell dilution at which growth occurs (MCD_{GROWTH}) in the presence and absence of each small molecule is scored by visual inspection. Any intrinsic effect of small molecule on bacterial growth is accounted for using a duplicate plate of bacteria expressing βla-linker, as described in **Supplementary Fig. 6** and online Methods. Note that at the single concentration of ampicillin used in the HTS format of the assay (100 μg/mL), 100 % rescue of bacterial growth gives rise to a $\log_2(\text{treated/untreated})$ of 2.
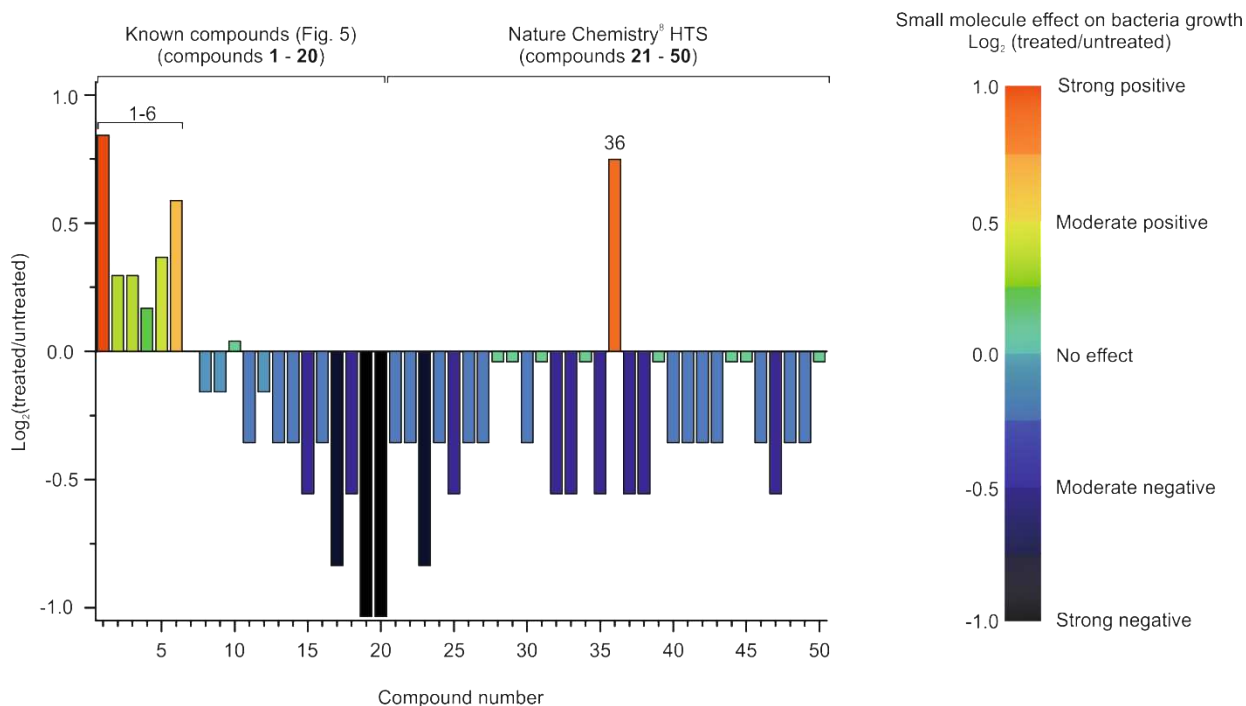
Supplementary Figure 9. High throughput format of *In vivo* screen of 50 compounds (100 μM compound and 100 μg/mL ampicillin) with known effects against hIAPP aggregation. Compounds **1–20** correspond to the wenty compounds reported in **Fig. 4** of this manuscript. Compounds **21–50** correspond to small molecules screened against hIAPP aggregation and their binding modes characterized by ESI-MS alone in Young, Saunders *et al.* (2015)[8]. Hit compounds from the *in vivo* screen are numbered and correspond to curcumin (**1**), acid fuchsin (**2**), EGCG (**3**), Fast green FCF (**4**), acridine orange (**5**) caffeic acid (**6**) and JCS-1 (**36**) (compound numbered 26 in reference 8). Colors correspond to classification of the effect of the small molecule on bacterial growth (see color key). Note that at the single concentration of ampicillin used in the HTS format of the assay (100 μg/mL), 100 % rescue of bacterial growth results in $\log_2$(treated/untreated) = 2.
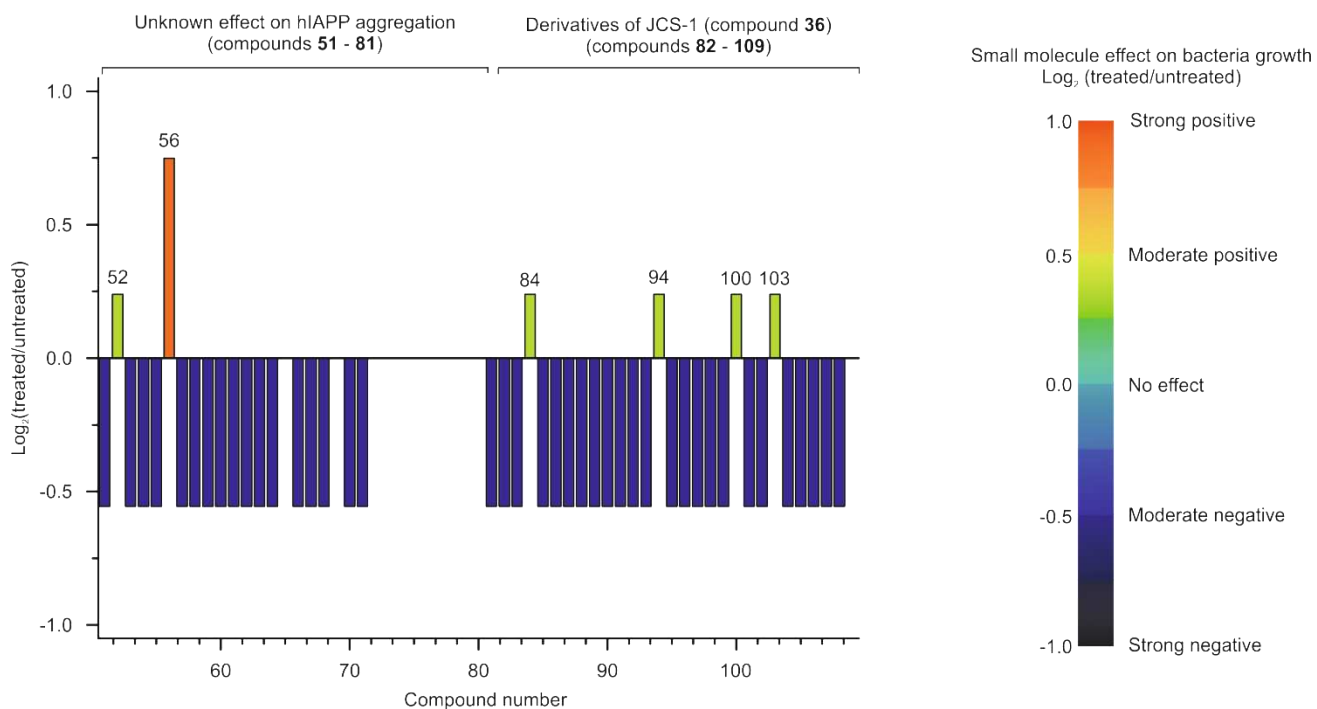
Supplementary Figure 10. *In vivo* screen of 59 novel compounds of βla-hIAPP aggregation (100 μM compound and 100 μg/mL ampicillin). Compounds **51-81** have known effects on the aggregation of other molecules, compounds **82** - **109** were chosen for analysis based on structural similarities to JCS-1 (compound **36**) shown here, and previously using ESI-MS and TEM[8], to inhibit hIAPP aggregation (see main text for details). Hit compounds from the *in vivo* screen are labeled by their number and colored by their effect on bacterial growth (see color key). Note that at the single concentration of ampicillin used in the HTS format of the assay (100 μg/mL), 100 % rescue of bacterial growth results in log_2(treated/untreated) = 2.
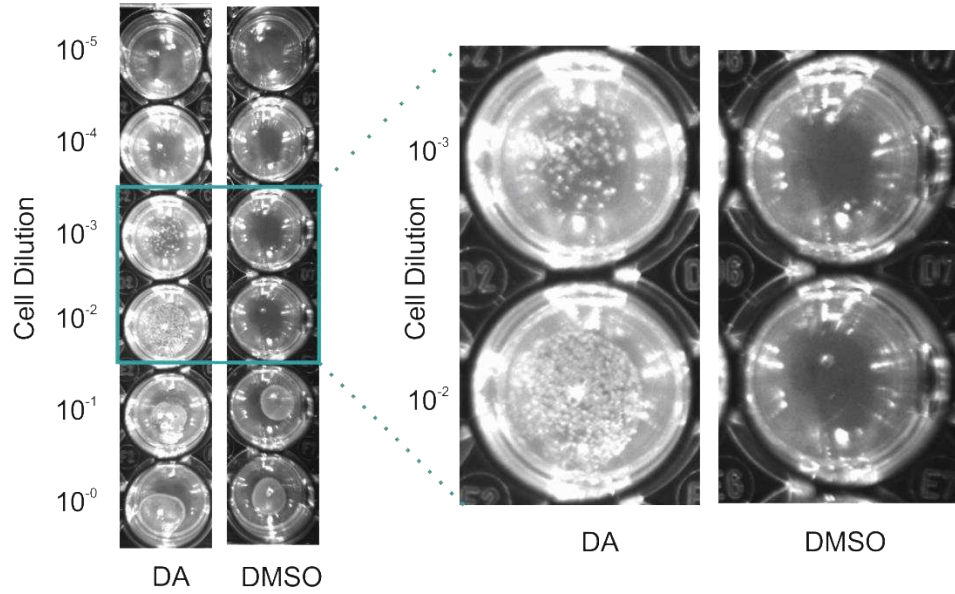
Supplementary Figure 11. Screen result for βla-hIAPP in the presence of 100 μM dopamine. *In vivo* assay plate showing the ability of colonies to grow in the presence of dopamine, or the control, DMSO (3 % *v/v*). In the presence of 100 μM dopamine, the maximal cell dilution at which growth occurs is 10^{-3} (in contrast to 10^{-1} in the absence of dopamine).
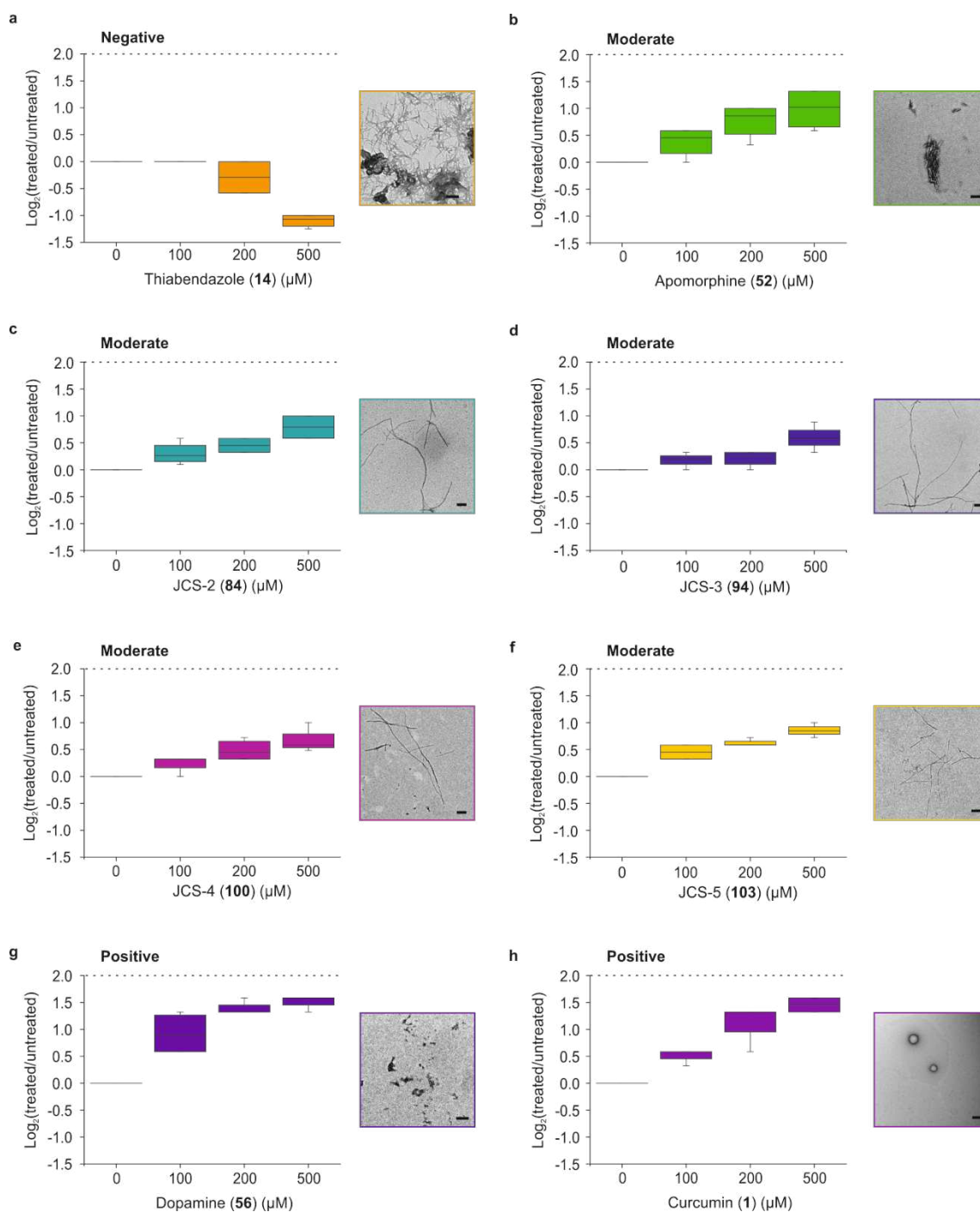
Supplementary Figure 12. Comparison of hits from HTS. Effect of increasing concentrations of hits from HTS on growth of bacteria expressing the βla-hIAPP construct compared with a compound that does not affect hIAPP aggregation (thiabenzadole) and a compound that prevents hIAPP aggregation (curcumin). Data for thiabendazole (**a**), the five moderate hits apomorphine (**b**), JCS-2 (**c**), JCS-3 (**d**), JCS-4 (**e**), JCS-5 (**f**), the strong hit dopamine (**g**) and curcumin (**h**) are plotted as $\log_2$(treated/untreated). High throughput format of assay was performed (single concentration of ampicillin, 100 µg/mL). Data plotted as Center line = median; box limits = 25th and 75th percentiles (whiskers extending to ± 1.5 x IQR), n = 4. Compound number is given in brackets. Data were plotted after the toxicity of the small molecule was accounted for by analysis of the effect of each concentration of small molecule on the growth of cells expressing βla-linker. At 100 µg/mL ampicillin, 100 % rescue gives $\log_2$(treated/untreated) = 2 (indicated by dotted line). Negative stain TEM analysis of hIAPP aggregation after 5 days incubation (pH 6.8, quiescent, 25 °C) of a 10:1 molar ratio (320:32 µM) of small molecule: hIAPP). Scale bar = 100 nm.
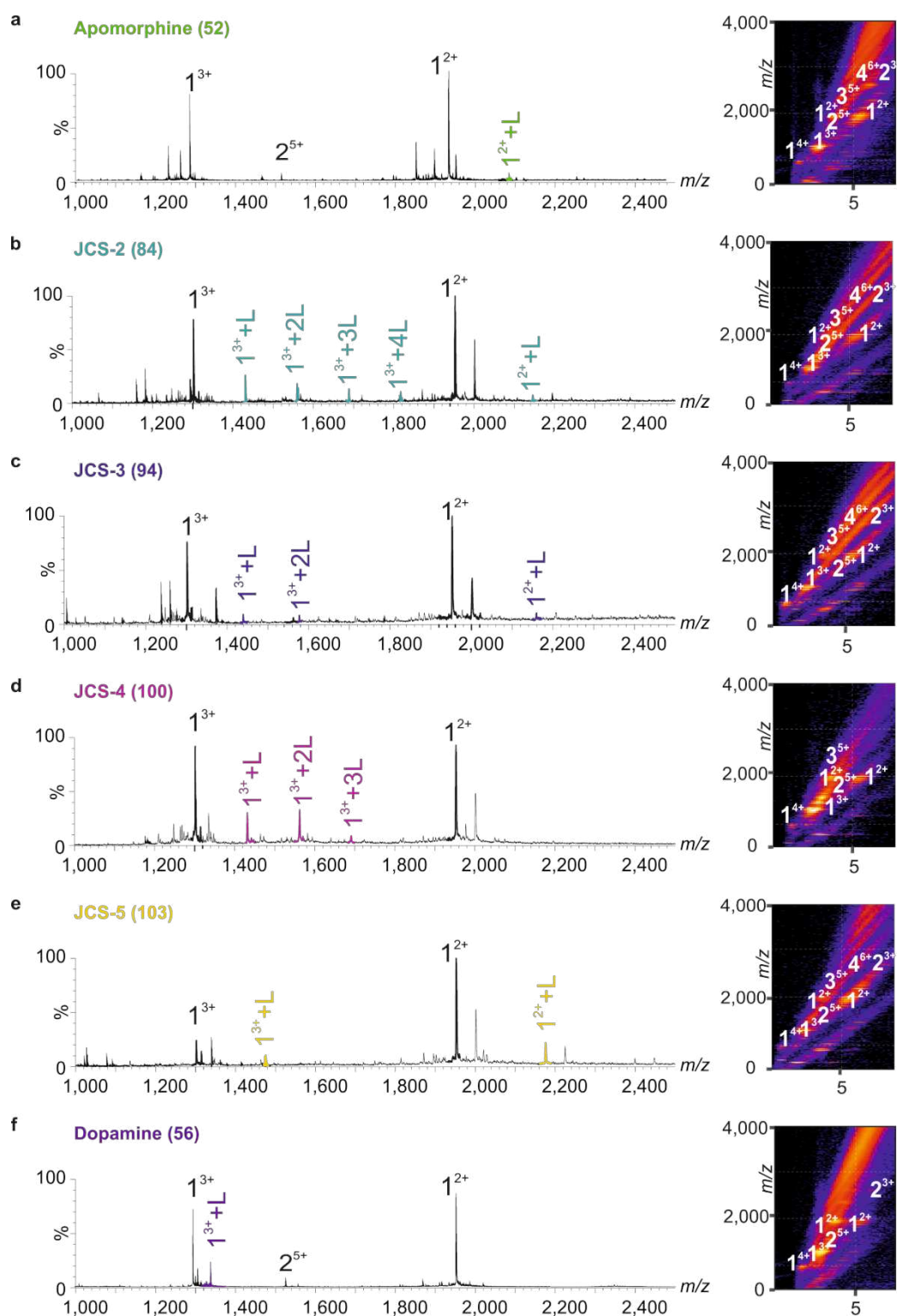
Supplementary Figure 13. Mass spectrometric analysis of hits from the HTS. ESI-IMS-MS mass spectra and Driftscope plots of hIAPP peptide in the presence of apomorphine (**a**), JCS-2 (**b**), JCS-3 (**c**) JCS-4 (**d**), JCS-5 (**e**) or dopamine (**f**). Compound number is given in brackets. Positive ion ESI mass spectra label X^{y+} denotes the oligomer order (X) and charge state of the species (y+). X^{y+} + nL denotes the number (n) of ligands (L) bound to the particular X^{y+} charge state. All *in vitro* experiments were performed with 32 μM hIAPP and 320 μM small molecule (pH 6.8, quiescent).
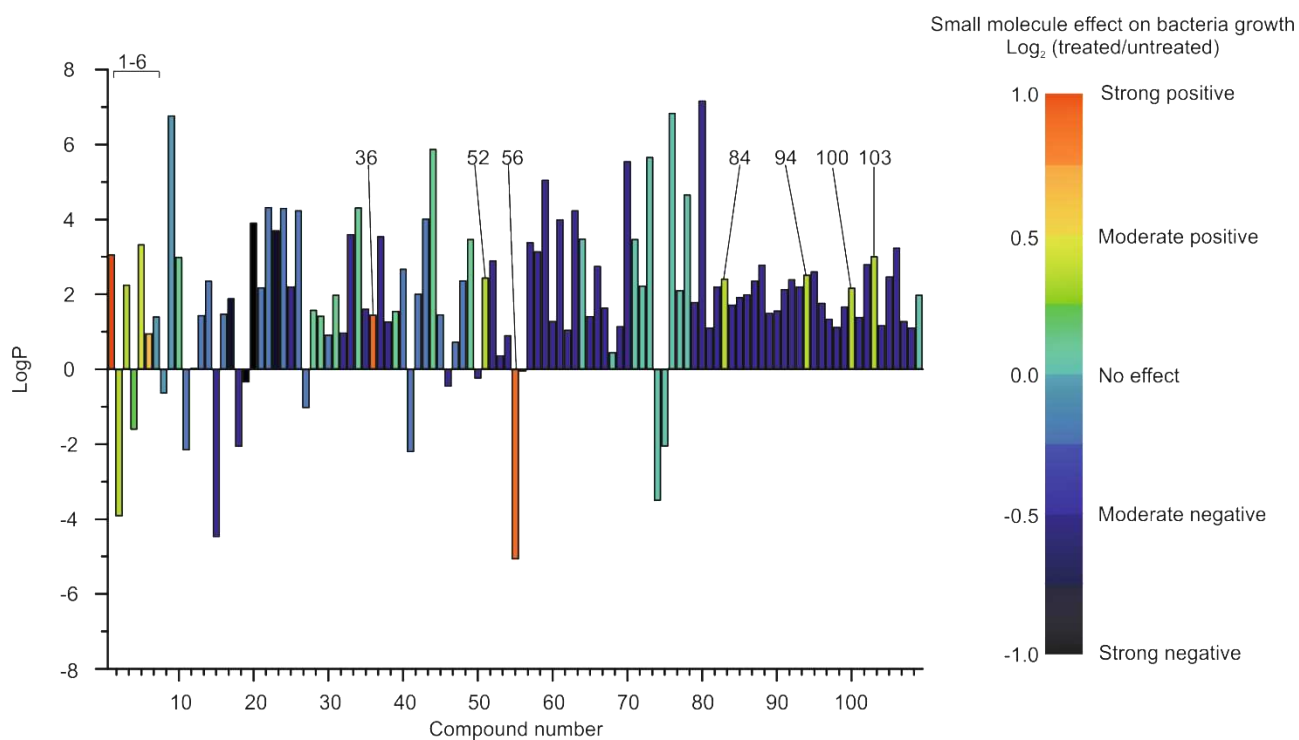
Supplementary Figure 14. LogP values of compounds screened. LogP values (the log of the hydrophobic/aqueous partition coefficient) of the small molecules were calculated using www.molinspiration.com software. Molecules with high positive LogP values have high hydrophobicity. Colors correspond to classification of the effect of the small molecule on bacterial growth from the HTS assay (see color key). *In vivo* hit molecules are indicated by their number.
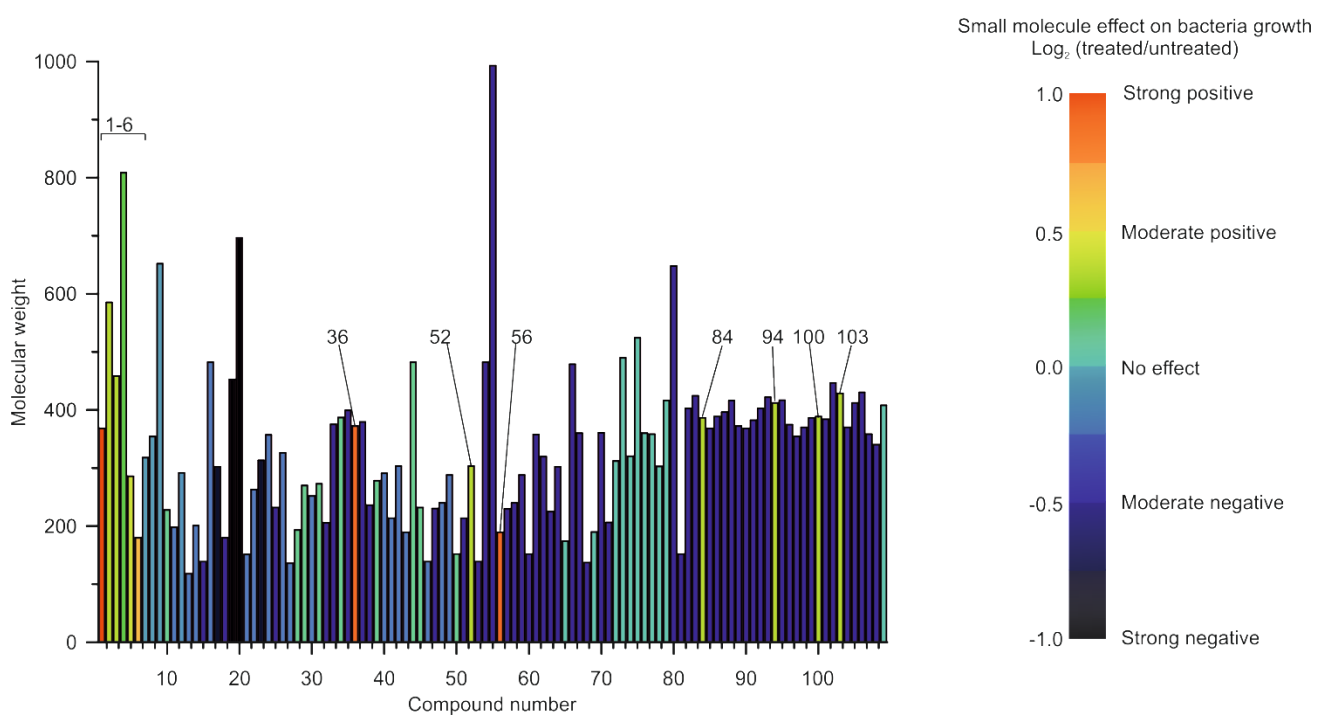
Supplementary Figure 15. Molecular weight of compounds screened. Colors correspond to classification of the effect of the small molecule on bacterial growth from the HTS assay (see color key). *In vivo* hit molecules are indicated by their number.

SUPPLEMENTARY RESULTS

Supplementary References

1. Daval, M. et al. The effect of curcumin on human islet amyloid polypeptide misfolding and toxicity. *Amyloid* **17**, 118-128 (2010).
2. Meng, F. & Raleigh, D.P. Inhibition of glycosaminoglycan-mediated amyloid formation by islet amyloid polypeptide and proIAPP processing intermediates. *J. Mol. Biol.* **406**, 491-502 (2010).
3. Meng, F. et al. The sulfated triphenyl methane derivative acid fuchsin is a potent inhibitor of amyloid formation by human islet amyloid polypeptide and protects against the toxic effects of amyloid formation. *J. Mol. Biol.* **400**, 555-566 (2010).
4. Young, L.M., Cao, P., Raleigh, D.P., Ashcroft, A.E. & Radford, S.E. Ion mobility spectrometry–mass spectrometry defines the oligomeric intermediates in amylin amyloid formation and the mode of action of inhibitors. *J. Am. Chem. Soc.* **136**, 660-670 (2013).
5. Palhano, F.L., Lee, J., Grimster, N.P. & Kelly, J.W. Toward the molecular mechanism(s) by which EGCG treatment remodels mature amyloid fibrils. *J. Am. Chem. Soc.* **135**, 7503-7510 (2013).
6. Cao, P. & Raleigh, D.P. Analysis of the inhibition and remodeling of islet amyloid polypeptide amyloid fibers by flavanols. *Biochem.* **51**, 2670-2683 (2012).
7. Kamihira-Ishijima, M., Nakazawa, H., Kira, A., Naito, A. & Nakayama, T. Inhibitory mechanism of pancreatic amyloid fibril formation: formation of the complex between tea catechins and the fragment of residues 22–27. *Biochem.* **51**, 10167-10174 (2012).
8. Young, L.M. et al. Screening and classifying small molecule inhibitors of amyloid formation using ion mobility spectrometry-mass spectrometry. *Nat. Chem.* **7**, 73-81 (2015).
9. Meng, F., Abedini, A., Plesner, A., Verchere, C.B. & Raleigh, D.P. The flavanol (-)-epigallocatechin 3-gallate inhibits amyloid formation by islet amyloid polypeptide, disaggregates amyloid fibrils, and protects cultured cells against IAPP-induced toxicity. *Biochem.* **49**, 8127-8133 (2010).
10. Cheng, B. et al. Coffee components inhibit amyloid formation of human islet amyloid polypeptide *in vitro*: possible link between coffee consumption and diabetes mellitus. *J. Agric. Food Chem.* **59**, 13147-13155 (2011).
11. Cheng, B. et al. Silibinin inhibits the toxic aggregation of human islet amyloid polypeptide. *Biochem. Biophys. Res. Commun.* **419**, 495-499 (2012).
12. Aitken, J.F., Loomes, K.M., Konarkowska, B. & Cooper, G.J.S. Suppression by polycyclic compounds of the conversion of human amylin into insoluble amyloid. *Biochem. J.* **374**, 779-784 (2003).
13. Aarabi, M.H. & Mirhashemi, S.M. The role of two natural flavonoids on human amylin aggregation. *Afr. J. Ph. Pharmacol.* **6**, 2374-2379 (2012).
14. Zelusa, C. et al. Myricetin inhibits islet amyloid polypeptide (IAPP) aggregation and rescues living mammalian cells from IAPP toxicity. *Open Biochem. J.* **6**, 66-70 (2012).
15. Noor, H., Cao, P. & Raleigh, D.P. Morin hydrate inhibits amyloid formation by islet amyloid polypeptide and disaggregates amyloid fibers. *Protein Sci.* **21**, 373-382 (2012).
16. Porat, Y., Mazor, Y., Efrat, S. & Gazit, E. Inhibition of islet amyloid polypeptide fibril formation: a potential role for heteroaromatic interactions. *Biochem.* **43**, 14454-14462 (2004).
17. Wu, C., Lei, H., Wang, Z., Zhang, W. & Duan, Y. Phenol red interacts with the protofibril-like oligomers of an amyloidogenic hexapeptide NFGAIL through both hydrophobic and aromatic contacts. *Biophys. J.* **91**, 3664-3672 (2006).
18. Tu, L.-H. et al. Mutational analysis of the ability of resveratrol to inhibit amyloid formation by islet amyloid polypeptide: critical evaluation of the importance of aromatic–inhibitor and histidine–inhibitor interactions. *Biochem.* **54**, 666-676 (2014).
19. Kim, Y.-S., Randolph, T.W., Manning, M.C., Stevens, F.J. & Carpenter, J.F. Congo red populates partially unfolded states of an amyloidogenic protein to enhance aggregation and amyloid fibril formation. *J. Biol. Chem.* **278**, 10842-10850 (2003).
20. Feng, B.Y. et al. Small-molecule aggregates inhibit amyloid polymerization. *Nat. Chem. Biol.* **4**, 197-199 (2008).

SUPPLEMENTARY RESULTS

21.   Meng, F., Marek, P., Potter, K.J., Verchere, C.B. & Raleigh, D.P. Rifampicin does not prevent amyloid fibril formation by human islet amyloid polypeptide but does inhibit fibril thioflavin-T interactions: implications for mechanistic studies of β-cell death. *Biochem.* **47**, 6016-6024 (2008).

22.   Walsh, D.M. et al. A facile method for expression and purification of the Alzheimer's disease-associated amyloid β-peptide. *FEBS J.* **276**, 1266-1281 (2009).

23.   Kabat, E.A., Wu, T.T., Perry, H.M., Gottesman, K.S. & Foeller, C. Sequences of proteins of immunological interest, Edn. 5th. (U.S. Department of Health and Human Services, Public Health Service, National Institutue of Health, Bethesda; 1991).